Title
SLIDING WEAR BEHAVIOR OF PROTECTIVE COATINGS FOR DIESEL ENGINE COMPONENTS

Author
Levy, A.

Publication Date
1984-04-01

Lawrence Berkeley Laboratory
UNIVERSITY OF CALIFORNIA

Materials & Molecular Research Division

Submitted to Wear

SLIDING WEAR BEHAVIOR OF PROTECTIVE COATINGS FOR DIESEL ENGINE COMPONENTS

A. Levy, D. Boone, E. January, and A. Davis

April 1984

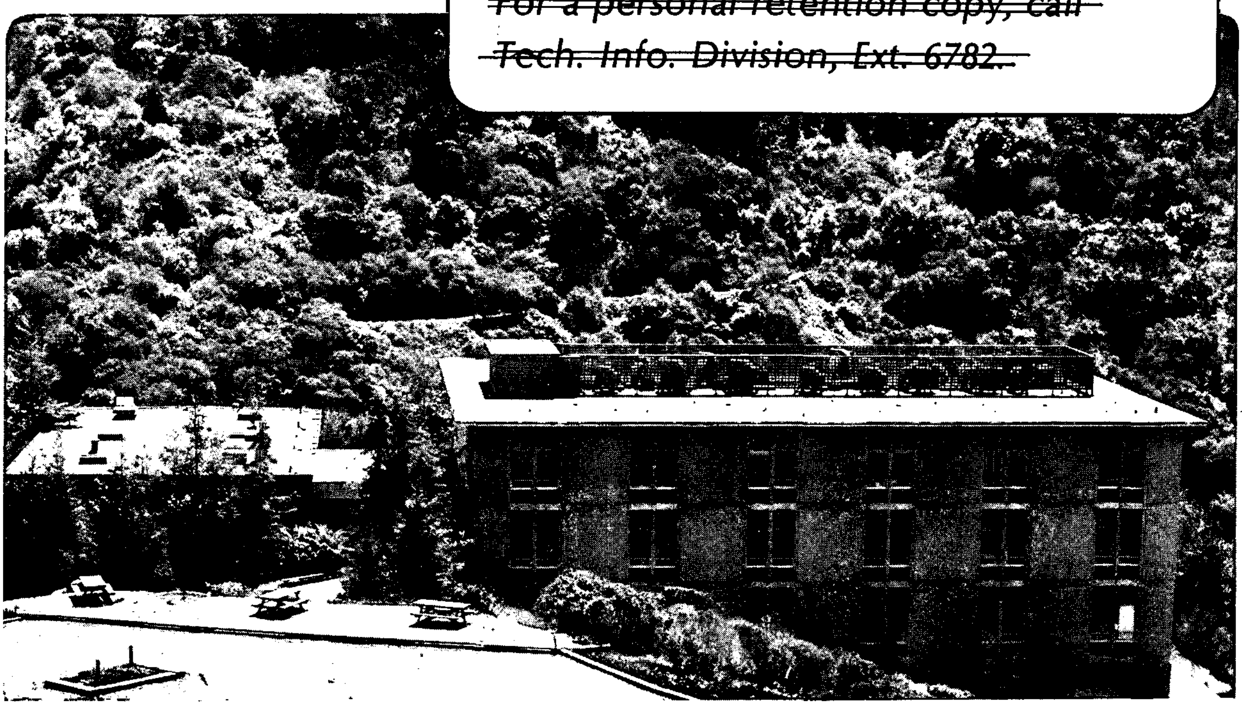

Prepared for the U.S. Department of Energy under Contract DE-AC03-76SF00098

LBL-17240

SLIDING WEAR BEHAVIOR OF PROTECTIVE COATINGS FOR DIESEL ENGINE COMPONENTS

Alan Levy, Donald Boone, Eric January and Anthony Davis

Materials and Molecular Research Division
Lawrence Berkeley Laboratory
University of California
Berkeley, California 94720

April 1984

This work was supported by the Assistant Secretary of Fossil Energy, Office of Coal Research, Heat Engines and Heat Recovery Division of the U.S. Department of Energy under Contract Number De-AC03-76SF00098 through the Battelle Memorial Institute, Pacific Northwest Laboratories, Richland, WA.

ABSTRACT

The use of heat insulating coatings on the cylinder walls of diesel engines is currently being considered for certain advanced engine designs. Since a major consideration in such an application is the wear resistance of the coatings, a series of tests has been carried out to determine the sliding wear behavior of several pairs of candidate materials systems. The tests were performed using a washer on disc specimen configuration and an oscillatory rotation movement to simulate the motion of a piston ring on a cylinder wall. It was determined that each material tested had a different pattern of sliding wear behavior. Chromium impregnating plasma sprayed Y_2O_3-ZrO_2 with chromia markedly improved its wear resistance.

INTRODUCTION

The use of protective coating systems on combustion chamber region components in advanced diesel engine designs is being contemplated for a number of reasons. They include permitting operation using degraded fuels, increasing durability and maintainability, increasing performance efficiency and reducing cooling requirements. The use of ceramic and hard metal coating systems on the cylinder walls and piston rings requires that detailed knowledge of the nature of the sliding wear behavior of potential pairs of materials be obtained.

The tests reported on herein were carried out on several of the more promising candidate materials systems for insulating the cylinder walls and for reducing friction and wear on the liners. The materials were tested against themselves in a washer and disc configuration and against a chromium plated washer at room temperature.

The basic wear rates and mechanisms that were determined provide an understanding of the relative sliding wear behavior of the materials tested and the mechanisms of surface degradation that are occurring. Tests will be run at elevated temperatures under the types of loads that can be experienced in service to establish wear rates that can be directly used in component design.

MATERIALS

The test coatings were obtained from suppliers who applied them on mild steel washers and discs for testing in a Falex 6 test device. Figure 1 is a drawing of the washer and disc. The contact surface area of the washer is 0.2 in^2. The larger disc has an area of 0.9 $in.^2$ surface area. The coatings were applied at various thicknesses that were appropriate for each material system. All of the coatings were tested in the as-applied surface condition without any surface grinding prior to testing and without lubrication.

The materials pairs tested in this series are listed in Table 1 along with the resulting wear rates, which will be discussed later. The materials systems are experimental coatings that are proprietary to the suppliers, hence only rudimentary compositions are reported. The Y_2O_3-ZrO_2, partially stabilized zirconia, ceramic thermal barrier coatings (CTBC) were all applied by plasma spraying. An MCrAlY bond coat was plasma sprayed on the solvent cleaned mild steel surfaces prior to deposition of the CTBC. Figure 2 are cross section micrographs at two magnifications of an unimpregnated Y_2O_3-ZrO_2 plasma sprayed coating, 0.28mm thick. Figure 3 are cross section micrographs at two magnifications of the Cr_2O_3 impregnated Y_2O_3-ZrO_2 coating, 0.56mm thick. The microstructure of the cast iron taken from a diesel engine cylinder wall is shown in Figure 4. The Cr plated steel washers had a standard chromium plating on them of the type used on piston rings in diesel engines.

TEST DESCRIPTION

Wear tests of the material pairs were conducted using the Falex-6 thrust washer testing machine. This device rotates or oscillates the surface of an upper rimmed washer against a stationary lower disc at a variety of speeds and contact pressures. The tests reported were conducted at 230 cycles per minute with the sliding direction reversed each 90° of rotation. Thus the rotation somewhat simulates the up and down motion of a piston ring on a cylinder wall.

A contact pressure is maintained between the specimens by means of a lever arm assembly which transfers a load of suspended weight to a static axial load action between the washer/disc pair. Three different contact pressures were used, 25, 50, and 100 psi. These pressures are lower than the peak contact pressures that occur in the piston ring-cylinder wall contacts in a diesel engine. The tests were carried out at room temperature with no lubrication. Each test was run for the number of minutes listed in Table 1. Periodically during the test the test was interrupted and the specimen was removed and weighed.

Preparation of the specimens for testing started with ultrasonic cleaning in a bath of ethanol for 5 minutes followed by thorough drying in forced hot air for 10 minutes. After each test increment, the specimens were cleaned by dry brushing prior to taking weight measurements.

The wear rates calculated from these sliding wear tests are incremental rates. The specimens were tested at short successive time increments ranging from 1 to 16 minutes in length, rather than testing for one longer time duration per material pair. The weight loss was measured after each time increment and the incremental wear rate was calculated as weight loss during the increment divided by the increment duration. Also, an average wear rate was calculated over the entire test duration for each pair.

RESULTS AND DISCUSSION

Each pair of materials tested had a distinct pattern of wear behavior. An analysis of Table 1 indicates several relationships among the materials tested:

1. When the coatings slide on themselves, the washer wears more than the disc.

2. A peak incremental wear rate occurs that is up to several times higher than the final wear rate.

3. The average incremental wear rate of the unimpregnated Y_2O_3-ZrO_2 relates directly with the contact pressure, reducing in half with each reduction of the contact pressure by half.

4. When the Y_2O_3-ZrO_2 is impregnated with chromia the wear rate decreases by an order of magnitude compared to the unimpregnated Y_2O_3-ZrO_2 coating. Also, the wear of the

coating is no longer a direct function of the contact pressure; the two higher pressures resulted in near the same amount of wear.

5. The chromium plating wears less than any of the other materials tested and its wear is independent of contact pressure.

6. When the washer is chromium plated, the pattern of wear of the Y_2O_3-ZrO_2 coatings changes. Now the disc with the coating on it wears more than the Cr plated washer.

7. Both the unimpregnated and impregnated Y_2O_3-ZrO_2 coatings wear the same amount when they are sliding against a Cr plated washer.

8. The cast iron has a low wear rate when it is paired against itself and a medium wear rate when paired against a Cr plated washer. It has better wear resistance than the impregnated Y_2O_3-ZrO_2 coating.

Curves of incremental wear rates for the materials tested show that at least three distinct curve shapes occurred. Analysis of these shapes indicates something about the mechanism of wear that is occurring. Further, detailed metallographic analysis and other refined testing is still required to verify the postulated reasons for the shapes of the curves. Such work is currently underway.

Figure 5 shows the incremental wear rate curve for the washer of the unimpregnated Y_2O_3-ZrO_2 pair sliding on itself at the three contact pressures. Note that there is a peak of wear that occurs at the higher two pressures and that a general trend exists (which is better defined in other wear pairs data) where the incremental wear starts at a higher level per increment of exposure and drops to a lower level at steady state conditions. The wear rate peak as well as the slope of the curve in the peak region decreases with a decrease in the contact pressure, essentially disappearing at the 25 psi pressure. For the two lower contact pressures the incremental wear rate reaches a steady state condition at 11 minutes of testing after which each time increment results in the same weight loss as the previous increment.

The reason for the higher initial wear rates can be seen in the photomicrographs in Figure 6 for the Y_2O_3-ZrO_2 coating tested at 50 psi contact pressure. Photo a shows the surface of the CTBC prior to testing. Photo b shows the worn surface after steady state wear was reached. It can be seen that the unworn, as deposited surface has many nodular protrusions that rise above the general surface plain. These protrusions are easier to remove than the material in the general plain of the surface and account for the higher initial incremental wear rate. Photo B shows the surface after steady state wear has been achieved. The much more planar surface wears at a lower rate.

The shape of the incremental wear curves are the same as those which were plotted for incremental erosion of Y_2O_3-ZrO_2 thermal barrier coatings in Reference 1. The reason established for the high initial incremental erosion rates in that study was the early removal of high protrusions of ceramic material that occur on the as-plasma sprayed surface. The same mechanism accounts for the higher initial wear rates observed in Figure 5.

Figure 7 shows the disc wear curves for the unimpregnated Y_2O_3-ZrO_2 pair. It can be seen that the wear that occurred on the wider surface disc was much lower than that which occurred on the narrow surface washer and it did not show a distinct wear peak as the washer did. The two lower contact pressures resulted in steady state wear rates essentially from the beginning of the test. The anomalous behavior of the 100 psi contact pressure curve is not explainable at this time.

Figure 8 shows the effect of the contact pressure on the wear rates of the washer and disc that were coated with unimpregnated Y_2O_3-ZrO_2.

The incremental wear rates of the Cr_2O_3 impregnated Y_2O_3-ZrO_2 pair sliding on itself are shown in Figure 9. It can be seen that the wear rates are much higher during the early part of the test and drop to much lower steady state rates. Unlike the curves for the unimpregnated Y_2O_3-ZrO_2 shown in Figure 5, the curves in Figure 9 show that the highest wear rate occurred on the washer that was tested at the lowest contact pressure, 25 psi. The two higher contact pressures resulted in the same, much lower incremental wear rates at steady state conditions. The direct effect of the lower contact pressures resulting in lower wear rates shown in Figure 5 can only be seen for the Cr_2O_3 impregnated Y_2O_3-ZrO_2 at the beginning of the tests. The initial incremental wear rate for the 25 psi contact pressure is considerably lower than the rates for the higher pressure tests.

The reason for the lowest contact pressure having the highest wear rate is thought to be due to a mechanism where individual voids with Y_2O_3-ZrO_2 walls that are impregnated with Cr_2O_3 break off near the beginning of each increment of the test and act as abrasive particles in a subsequent 3 body wear test mode. The 25 PSI is a low enough pressure to keep them from being crushed between the two sliding surfaces. Figure 10 shows these particles on the wear surface. Compare Figure 10 with Figure 6b. The voids seen in Figure 6b are filled in with the Cr_2O_3 as shown in Figure 10.

At the 50 and 100 psi contact pressures, the Cr_2O_3 impregnated, Y_2O_3-ZrO_2 abrasive particles are crushed to a much smaller size as soon as they are broken off the wear surface, a size where they do not act as abrasive particles in a classic 3 body wear situation. In effect, they act as a solid lubricant, eliminating the effect of the contact pressure difference on the wear rate.

Figure 11 further substantiates the 3 body wear premise. It shows the disc wear of the Cr_2O_3 impregnated Y_2O_3-ZrO_2 coating. The fact that the wear for the 25 psi contact pressure tests starts low and increases above the curves for the 50 and 100 psi contact pressure tests relates to the need to first break off the protruding particles on the more wear-prone washer surface as well as those on the lower wear rate disc before the system can wear in a 3 body abrasive wear mode. The lack of a steeply descending curve for the 25 psi test of the washer at the beginning of the test shown in Figure 9 correlates well with the slow start on the wear of the disc in the same test. The wear peaks which occur for all contact pressures are not explainable at this time. The effect of the higher contact pressure causing more wear than the lower pressure, as was observed in Figure 5 for the unimpregnated Y_2O_3-ZrO_2, can be seen by comparing the curves for the 50 and 100 psi pressures in Figure 11.

Figure 12 plots the wear rates as a function of contact pressure for the Cr_2O_3 impregnated Y_2O_3-ZrO_2 at 33 minutes of wear and clearly shows the higher rate at the 25 psi contact pressure and the same, lower rate for the 50 and 100 psi tests. At shorter wear times, a difference existed between the wear rates of the disc at 50 and 100 psi contact pressure.

Figure 13 shows how the Cr plated steel affects the wear patterns of the unimpregnated and impregnated Y_2O_3-ZrO_2 at the 50 PSI contact pressure. The shapes of these incremental wear rate curves combines the high starting rate and the peak rate curve shapes seen in the previous figures. Both types of ceramic coated discs follow the same pattern throughout the test duration and wear at the same rate. The wear rate of the unimpregnated Y_2O_3-ZrO_2 was reduced compared to its value when sliding on itself as shown in Figure 5. This indicates the detrimental effect that porosity has on sliding wear behavior. When one side of the pair is not porous, the wear potential of the pair is markedly reduced. The wear rate of the Cr_2O_3 impregnated ZrO_2 disc at the 50 psi contact pressure is 6 times greater than it is when sliding on itself as shown in Figure 11. The Cr plated steel washers (lower curves) wear very little throughout the test.

The pairing of these materials against the Cr plated steel washer had the effect of integrating the distinct wear pattern characteristics found when each material was paired against itself. The wear pattern observed combined the high initial rate with the mid-test peak rate and the corresponding wear rates fell somewhat in the mid-range between the higher wear rate of the unimpregnated Y_2O_3-ZrO_2 pair and the lower wear rate of the chromia impregnated Y_2O_3-ZrO_2 pair.

Figure 14 compares the higher wear rate Cr_2O_3 impregnated Y_2O_3-ZrO_2 coating sliding on itself with the low rate cast iron against itself and against Cr plated steel. The cast iron washer sliding on itself has a comparative wear rate to the Cr plated washer sliding on the cast iron. The fact that the Cr_2O_3 impregnated Y_2O_3-ZrO_2 wears at a rate only three times greater than the cast iron at steady state conditions indicates that it has considerable potential as a wear resistant coating as well as a thermal barrier coating.

Figure 15 shows a comparison between Cr_2O_3 impregnated Y_2O_3-ZrO_2 wearing on itself and on Cr plated steel. The highest curve is the ceramic coated disc wearing on a Cr plated steel washer. The lowest curve is a Cr plated washer. The open circle curve of the disc of the pair where both surfaces are ceramic coated should be compared to the open triangle curve of the ceramic coated disc wearing on Cr plated steel. There is a large difference in the wear rates that results from the great increase in the wear resistance of the Cr plating on the washer.

CONCLUSIONS

1. Cr plated steel as is currently used in diesel engines was the most wear resistant material tested.

2. Cr_2O_3 impregnating a plasma sprayed Y_2O_3-ZrO_2 CTBC reduced the sliding wear rate of the CTBC by an order of magnitude.

3. At the low contact pressure of 25 PSI the Cr_2O_3 impregnated voids in the Y_2O_3-ZrO_2 broke off the coating surface and acted as particles in a 3 body abrasive wear mode with a higher resultant wear rate.

4. The crushed, Cr_2O_3 impregnated voids of the Y_2O_3-ZrO_2 at the higher contact pressures acted as a solid film lubricant, eliminating the effect of contact pressure between 50 and 100 PSI.

5. When chromium plated washers were paired with ceramic coated discs, both the unimpregnated and Cr_2O_3 impregnated Y_2O_3-ZrO_2 coatings wore at the same rate, compared to an order of magnitude difference when each is rubbed on itself.

6. Porosity is very detrimental to the wear resistance of a ceramic coating.

REFERENCES

1. Levy, A., Boone, D., Davis, A. and Scholz, E., "The Erosion Protective Coatings", Proceedings 6th International Conference Erosion by Liquid and Solid Impact, Cambridge, England, September, 1983.

FIGURES

Table 1

Materials Pair		Peak Incremental Wear Rate [10^{-4} g/sec]			Final Incremental Wear Rate [10^{-4} g/sec]			Avg. Incremental Wear Rate [10^{-4} g/sec]			Test Duration (min)
		100psi	50psi	25psi	100psi	50psi	25psi	100psi	50psi	25psi	
1) Washer:	PT013 Y_2O_3-ZrO_2	4.5	2.3	1.4	2.2*	1.6**	0.6	3.22	1.80	0.72	16
Disc:	PT013 Y_2O_3-ZrO_2	1.8	0.85	0.5	1.8*	0.7**	0.25	1.40	0.66	0.33	16
2) Washer:	Cr_2O_3 impregnated Y_2O_3-ZrO_2	0.70	0.83	0.55	0.13	0.12	0.38	0.172	0.177	0.384	33
Disc:	Cr_2O_3 impregnated Y_2O_3-ZrO_2	0.33	0.20	0.28	0.03	0.05	0.16	0.106	0.071	0.179	33
3) Washer:	Cr plated 1018 steel	-	0.10	-	-	0.02	-	-	0.01	-	33
Disc:	PT037 Y_2O_3-ZrO_2	-	1.00	-	-	0.35	-	-	0.42	-	33
4) Washer:	Cr plated 1018 steel	-	0.07	-	-	0.01	-	-	0.02	-	33
Disc:	Cr_2O_3 impregnated Y_2O_3-ZrO_2	-	1.03	-	-	0.30	-	-	0.39	-	33
5) Washer:	Cr plated 1018 steel	0.17	-	-	0.02^{Δ}	-	-	0.01	-	-	27
Disc:	SiC particle impregnated 1018 steel	0.46	-	-	0.03	-	-	0.11	-	-	27
6) Washer:	SiC particle impregnated 1018 steel	0.12	-	-	0.03	-	-	0.04	-	-	27
Disc:	SiC particle impregnated 1018 steel	0.12	-	-	0.06	-	-	0.05	-	-	27

* Failed at 11 min.

** Failed at 16 min.

Δ Disregarded last weight measurement.

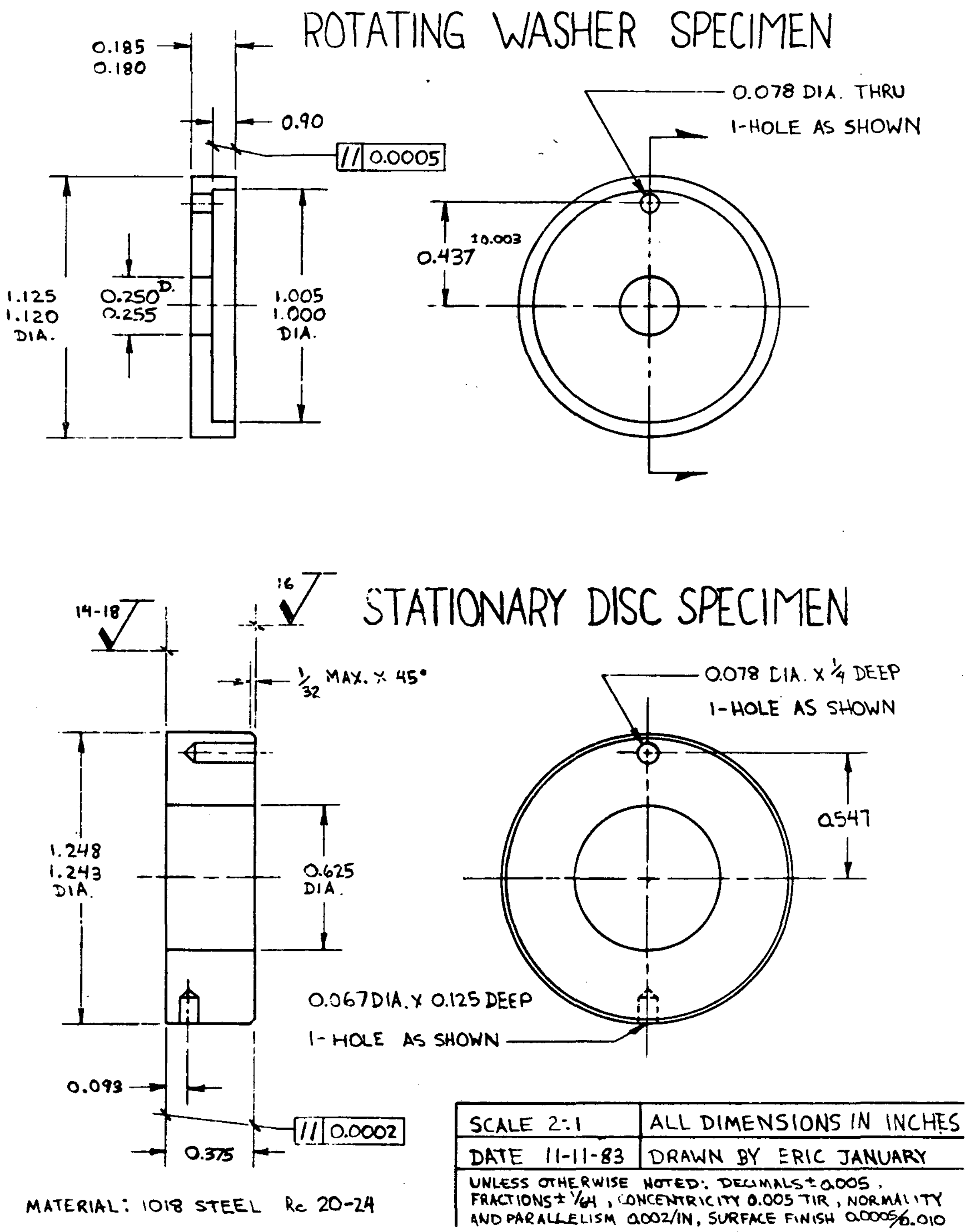

XBL 8311-4570

Fig. 1. Drawing of test washer and disc

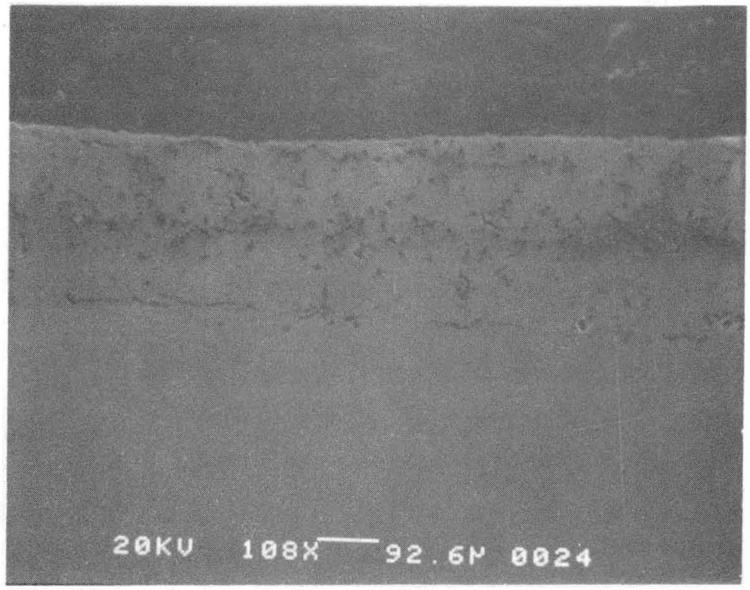

95 µm

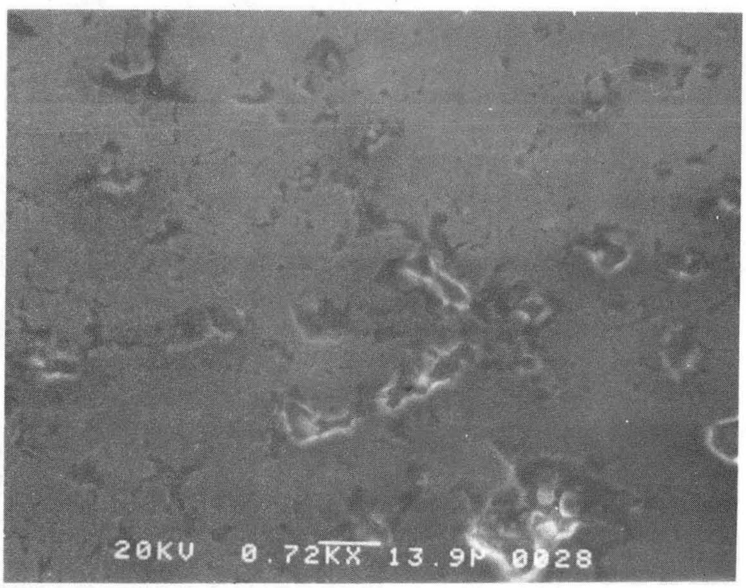

Fig. 2. Cross section of unimpregnated Y_2O_3-ZrO_2 coating

15 µm

XBB 841-473

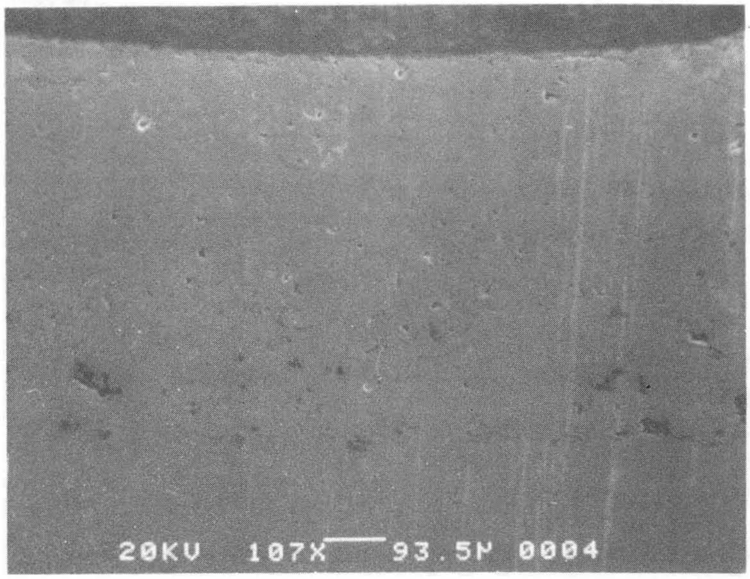

95 μm

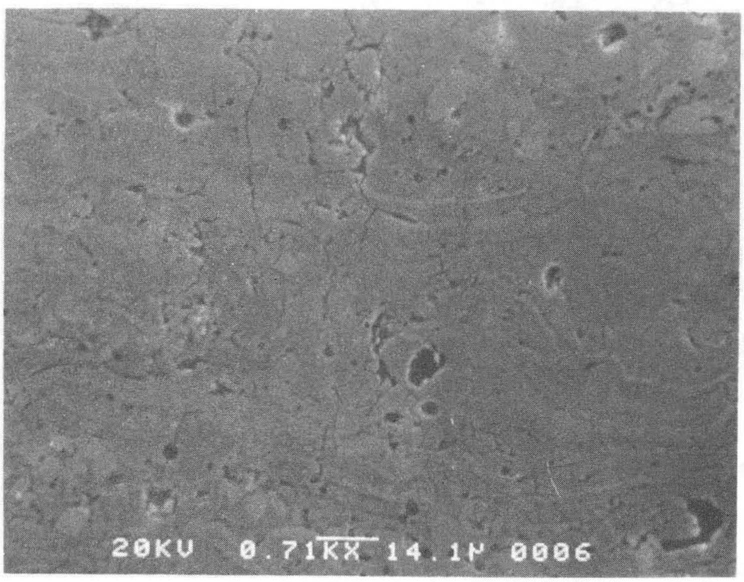

15 μm

Fig. 3. Cross section of Cr_2O_3 impregnated Y_2O_3-ZrO_2 coating

XBB 841-472

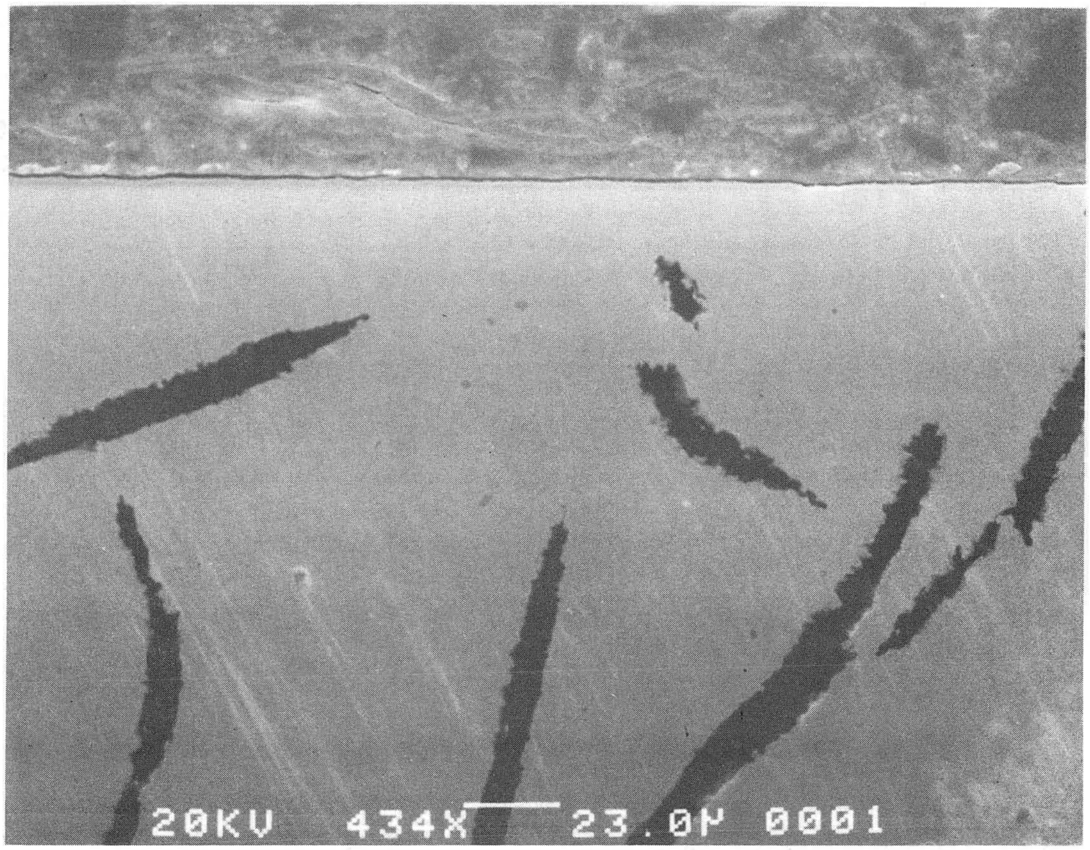

25 μm

Fig. 4. Cross section of cast iron cylinder wall

XBB 841-474

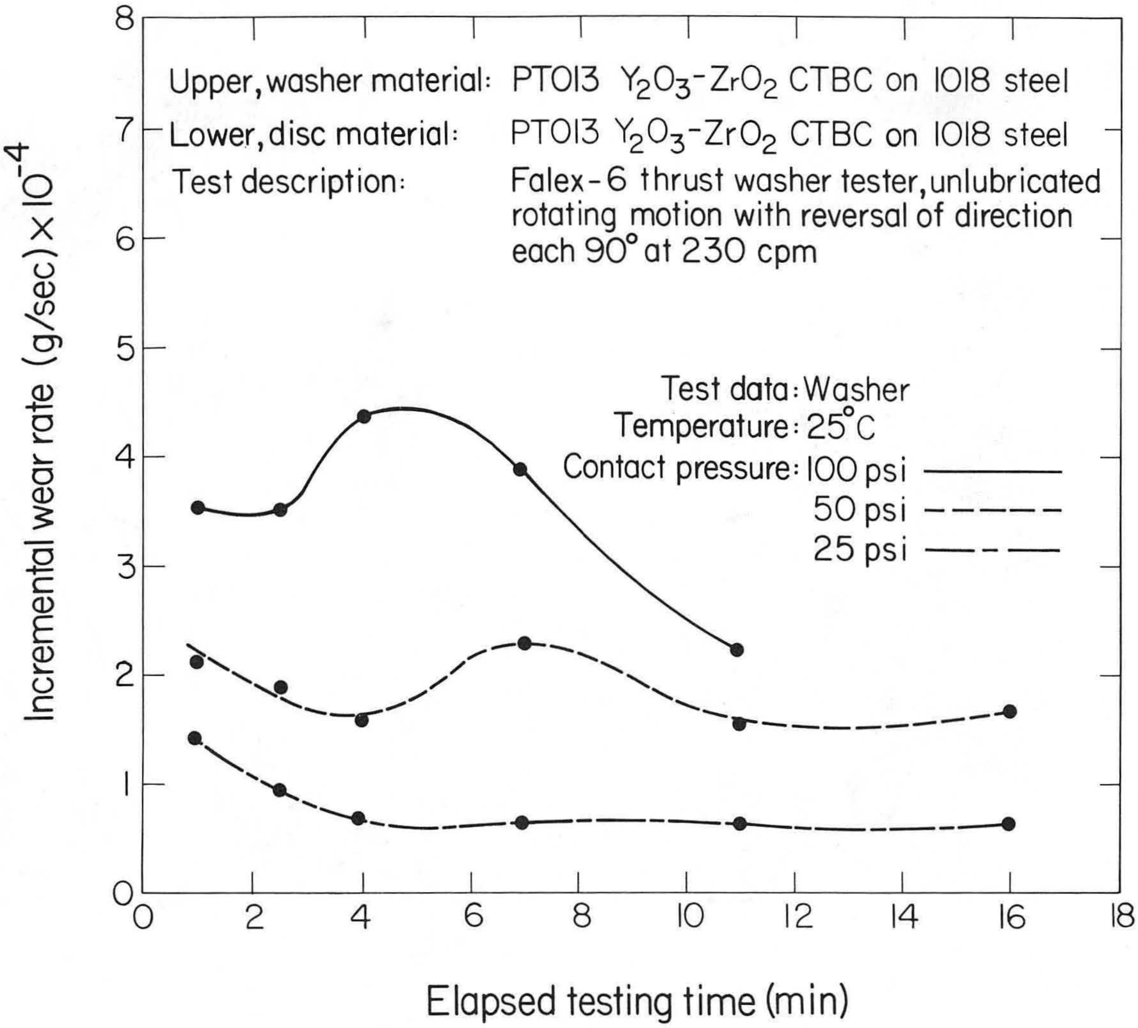

Fig. 5. Incremental wear rate of Y_2O_3-ZrO_2 CTBC on washer of 1018 steel

XBL 839-11818A

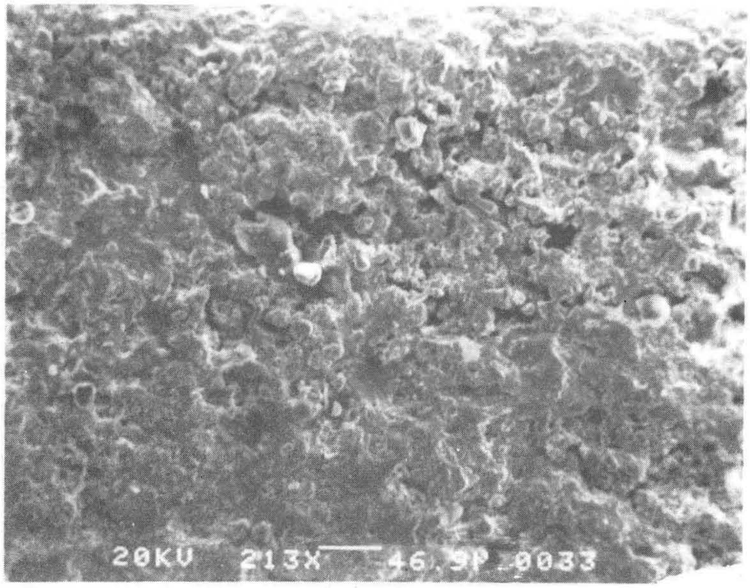

50 µm

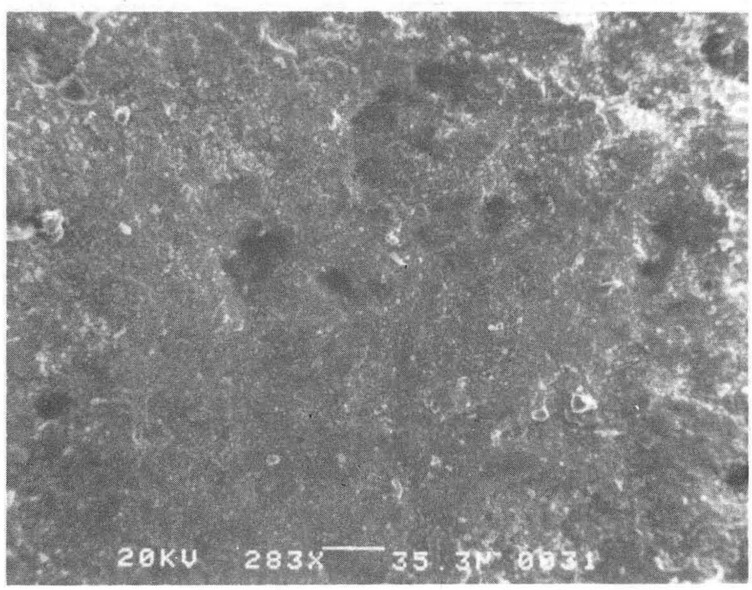

35 µm

Fig. 6. Surface of unimpregnated Y_2O_3-ZrO_2
(a) before and (b) after testing

XBB 841-475

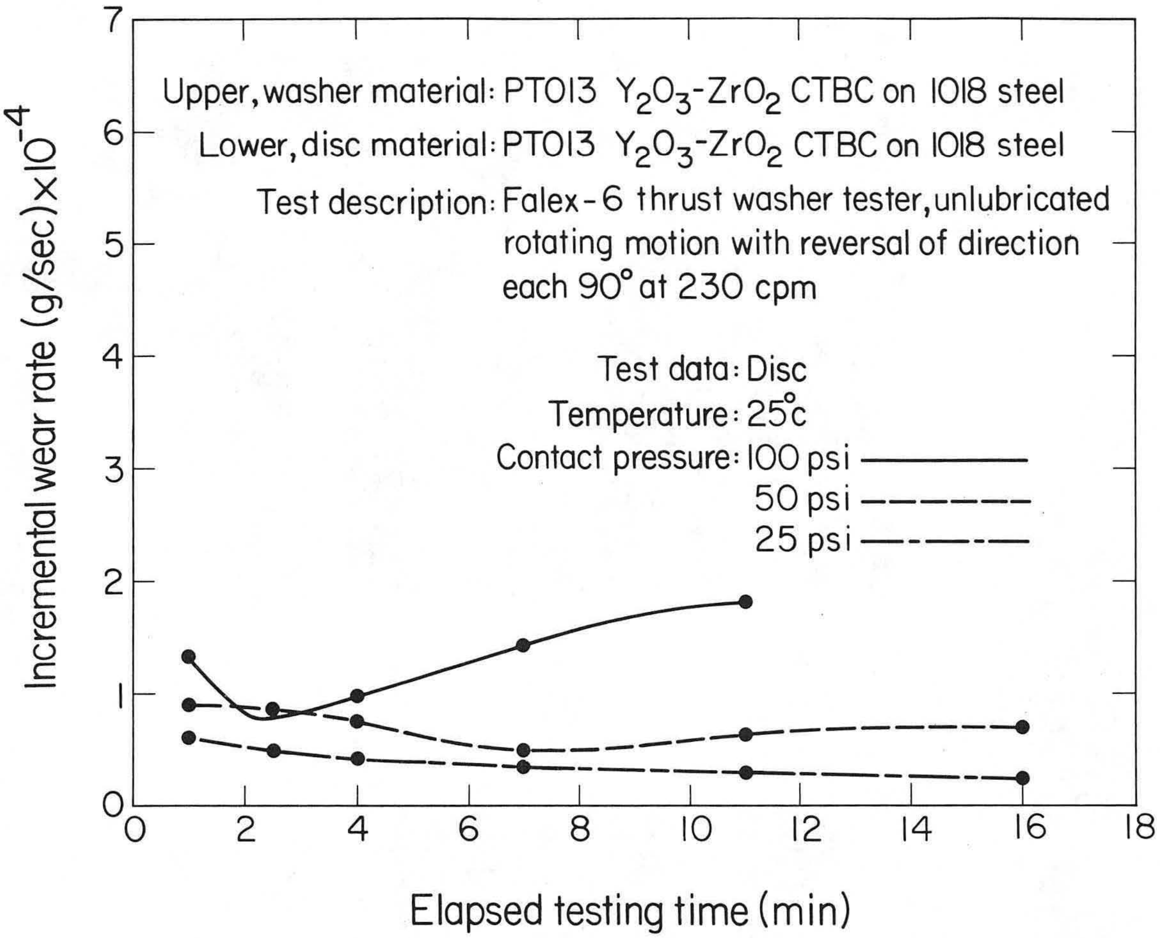

Fig. 7. Incremental wear rate of Y_2O_3-ZrO_2 CTBC on disc of 1018 steel

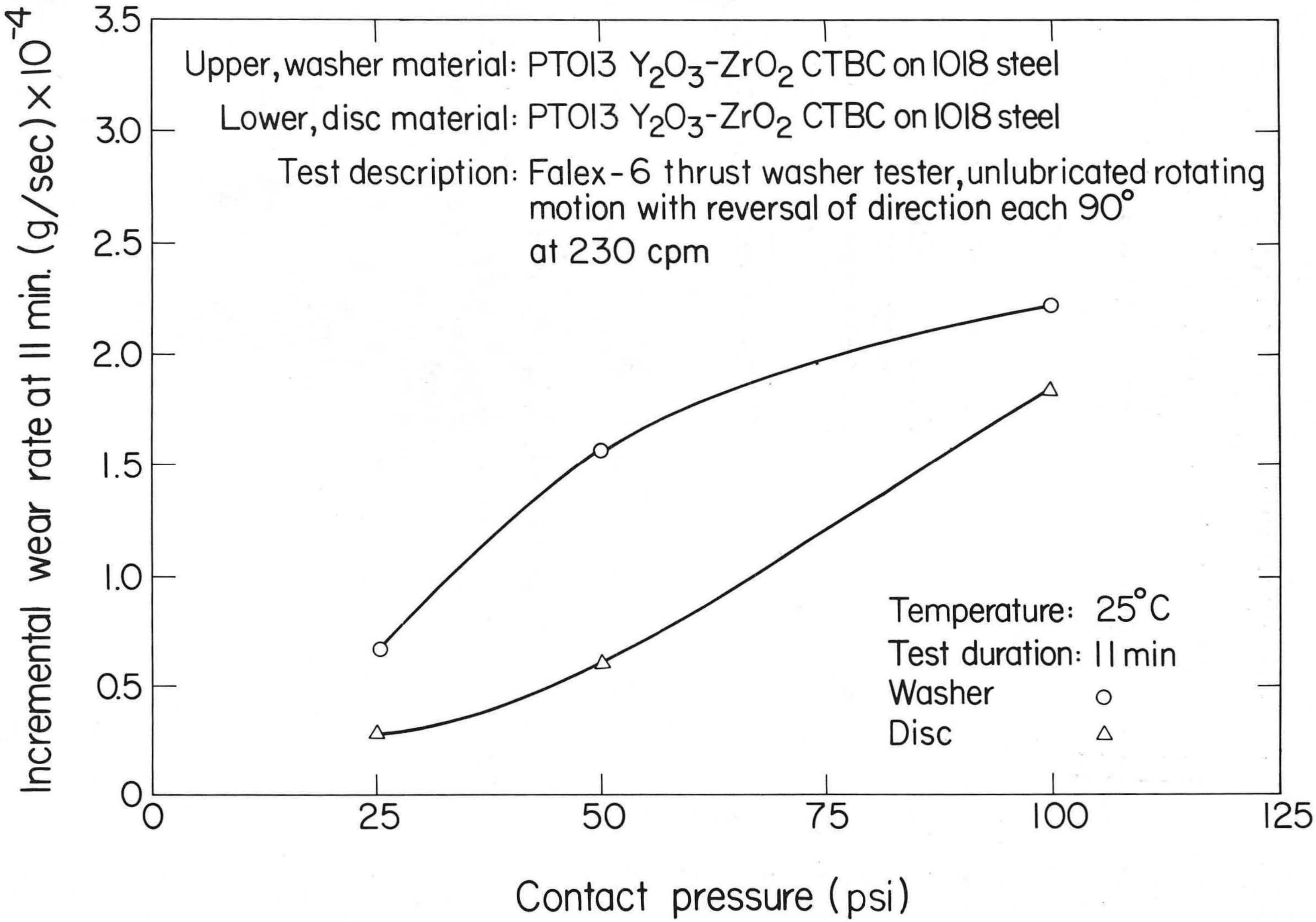

Fig. 8. Incremental wear rate vs contact pressure for Y_2O_3-ZrO_2 CTBC on 1018 steel

XBL 839-11823A

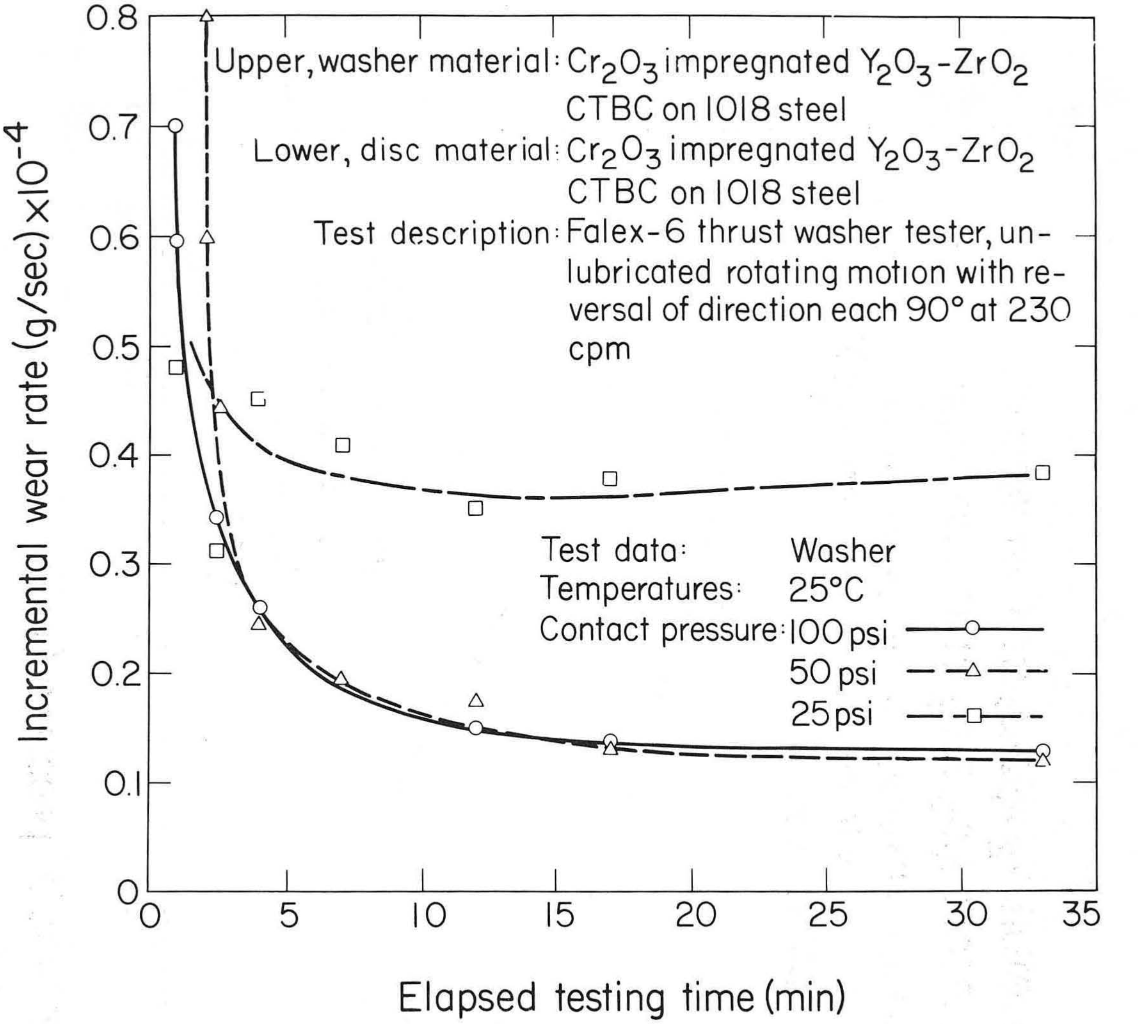

Fig. 9. Incremental wear rate of Cr_2O_3 impregnated Y_2O_3-ZrO_2 CTBC on washer of 1018 steel

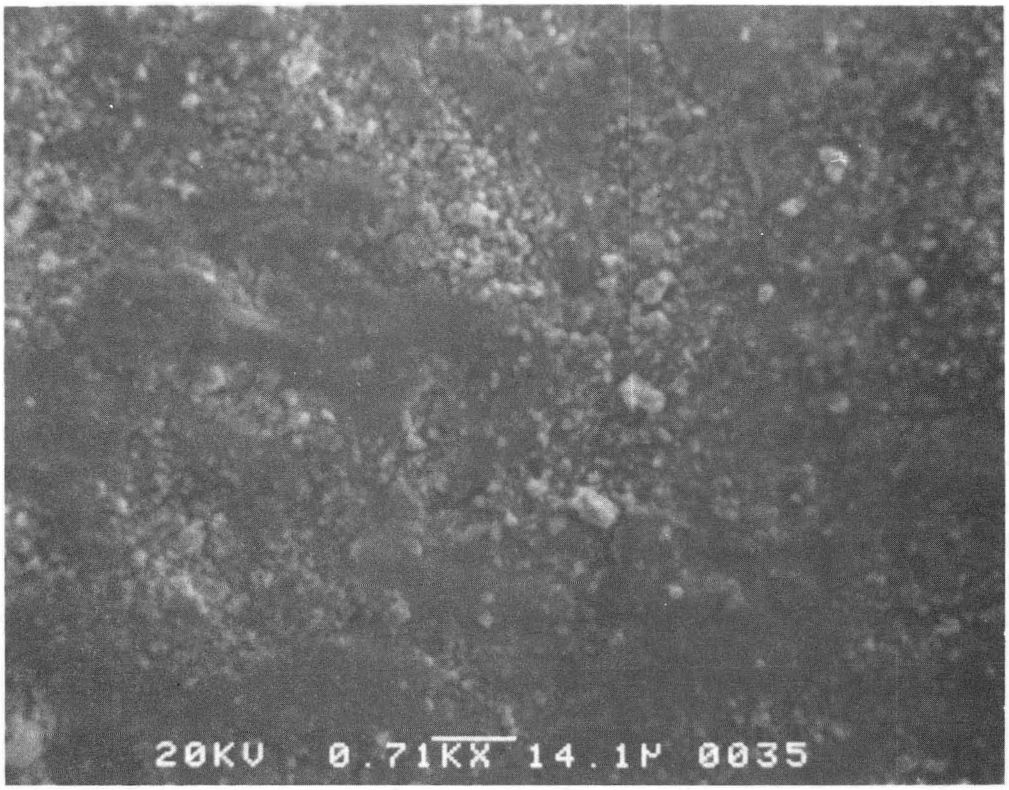

15 μm

Fig. 10. Tested surface of Cr_2O_3 impregnated Y_2O_3 -ZrO_2 tested at 25 psi contact pressure

XBB 841-476

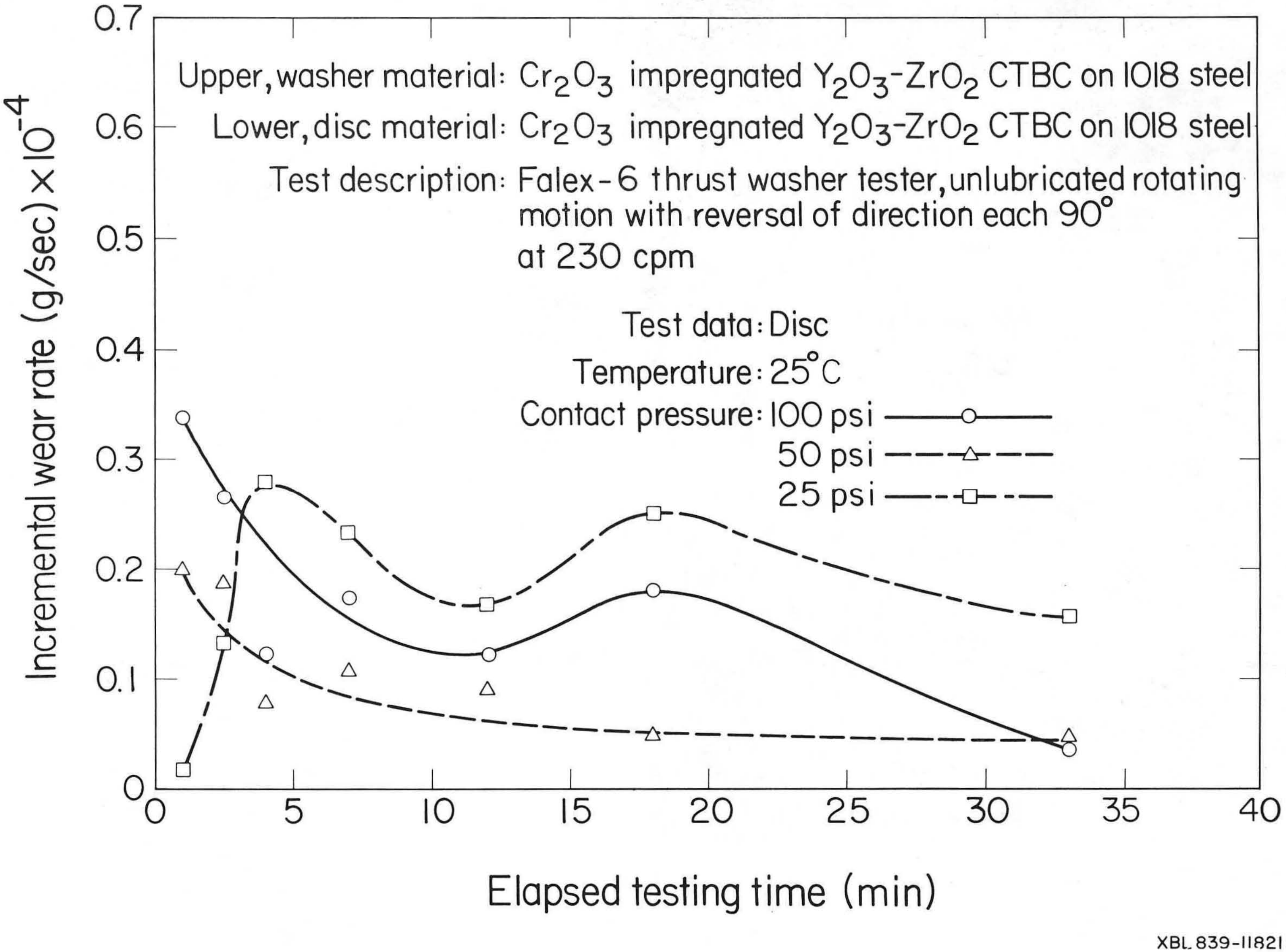

Fig. 11. Incremental wear rate of Cr_2O_3 impregnated Y_2O_3-ZrO_2 CTBC on disc of 1018 steel

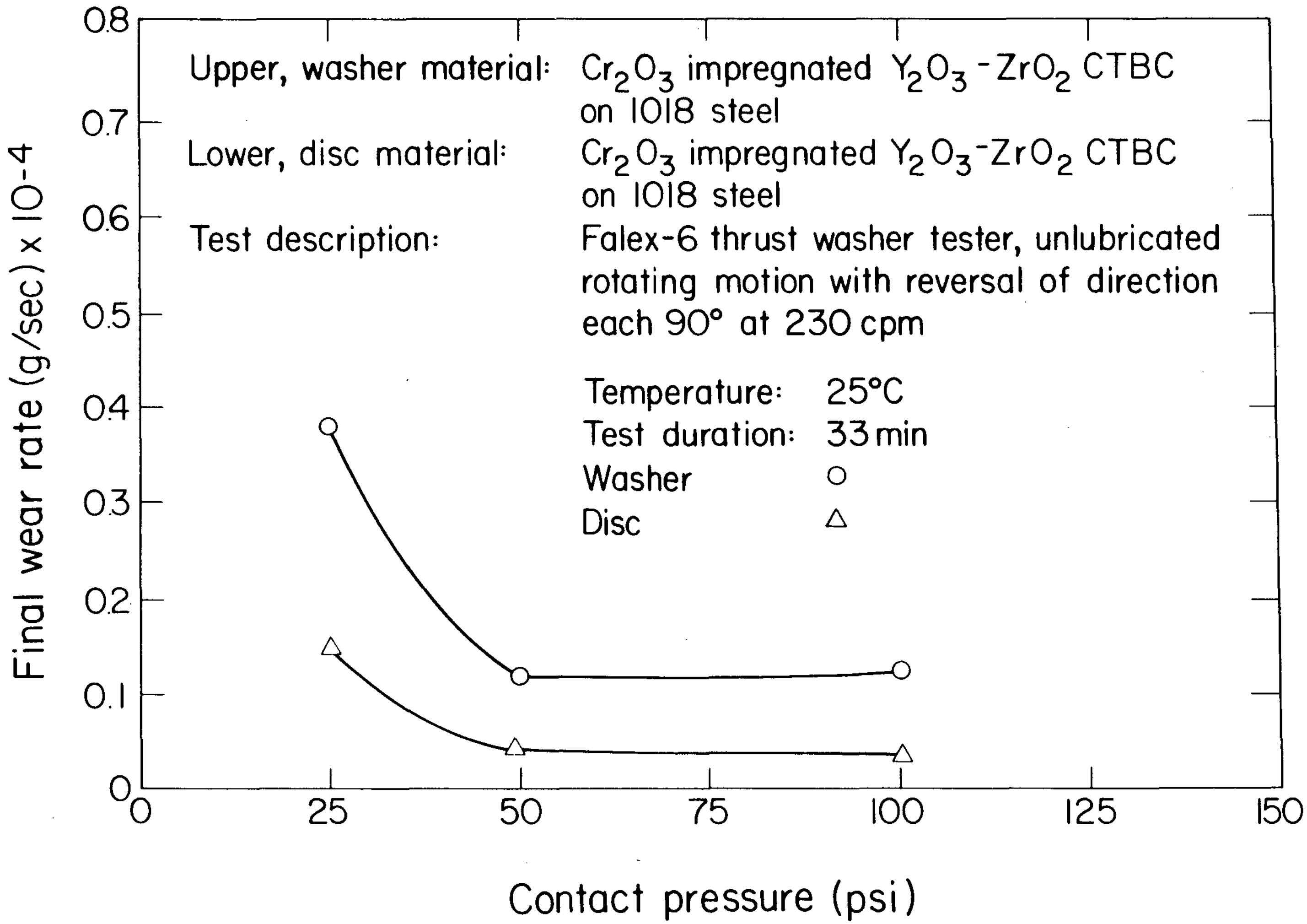

XBL 839-11819A

Fig. 12. Incremental wear rate vs contact pressure for Cr_2O_3 impregnated Y_2O_3-ZrO_2 CTBC on 1018 steel

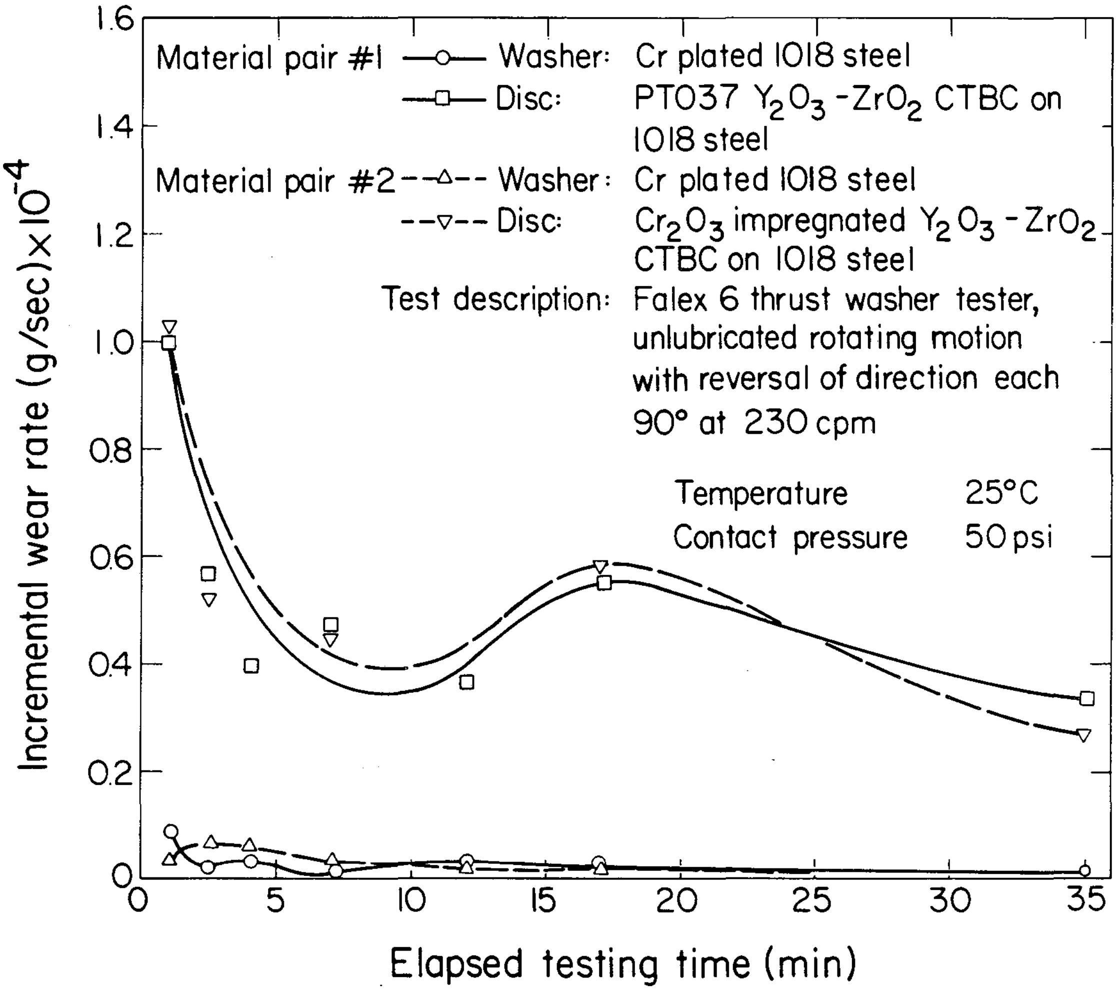

Fig. 13. Incremental wear rates of Cr plated washers and Y_2O_3-ZrO_2 and Cr_2O_3 impregnated Y_2O_3-ZrO_2 on discs of 1018 steel

XBL 839-11822A

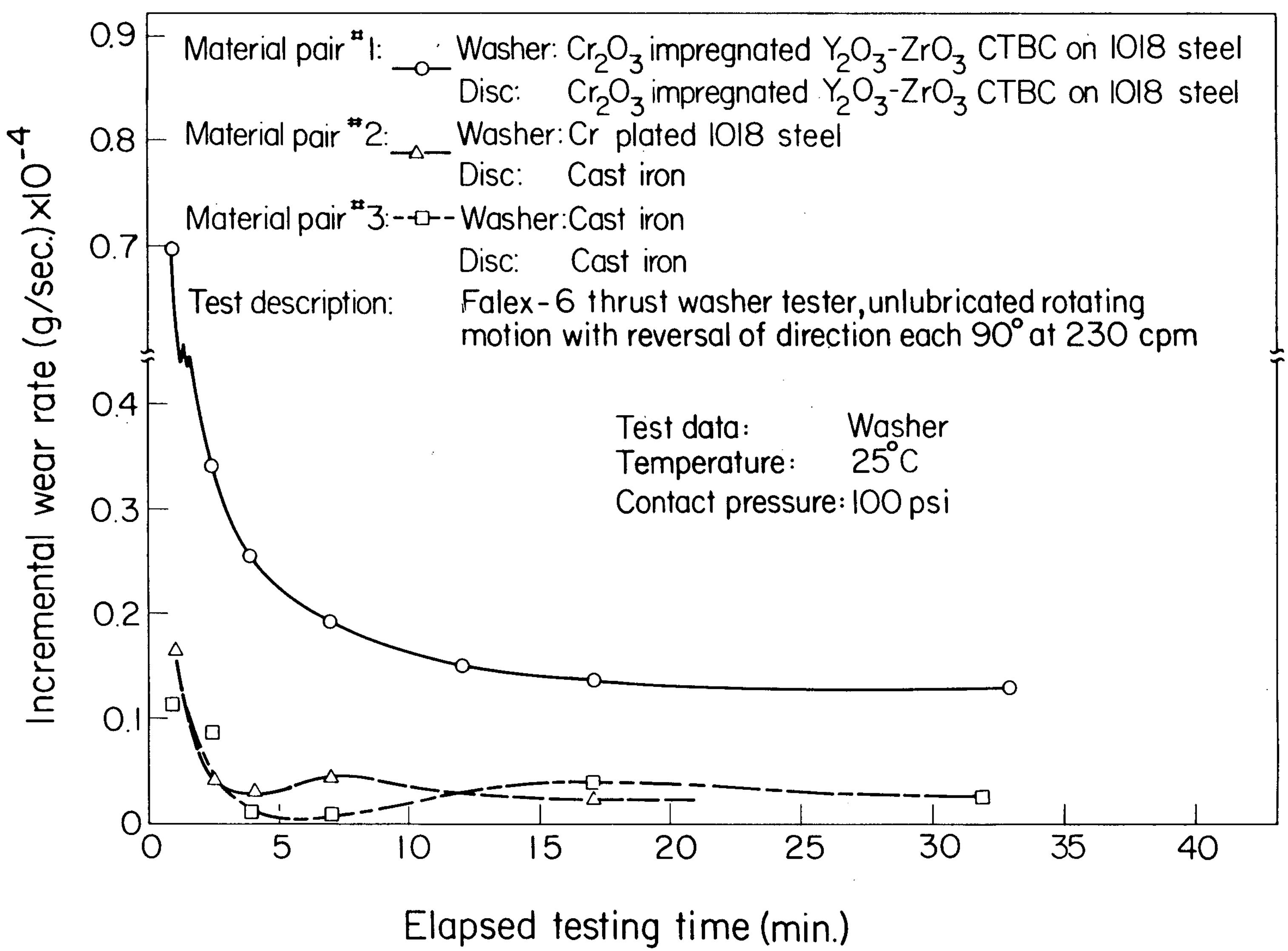

XBL 839-11820A

Fig. 14. Incremental wear rates of cast iron and Cr_2O_3 impregnated Y_2O_3-ZrO_2 CTBC

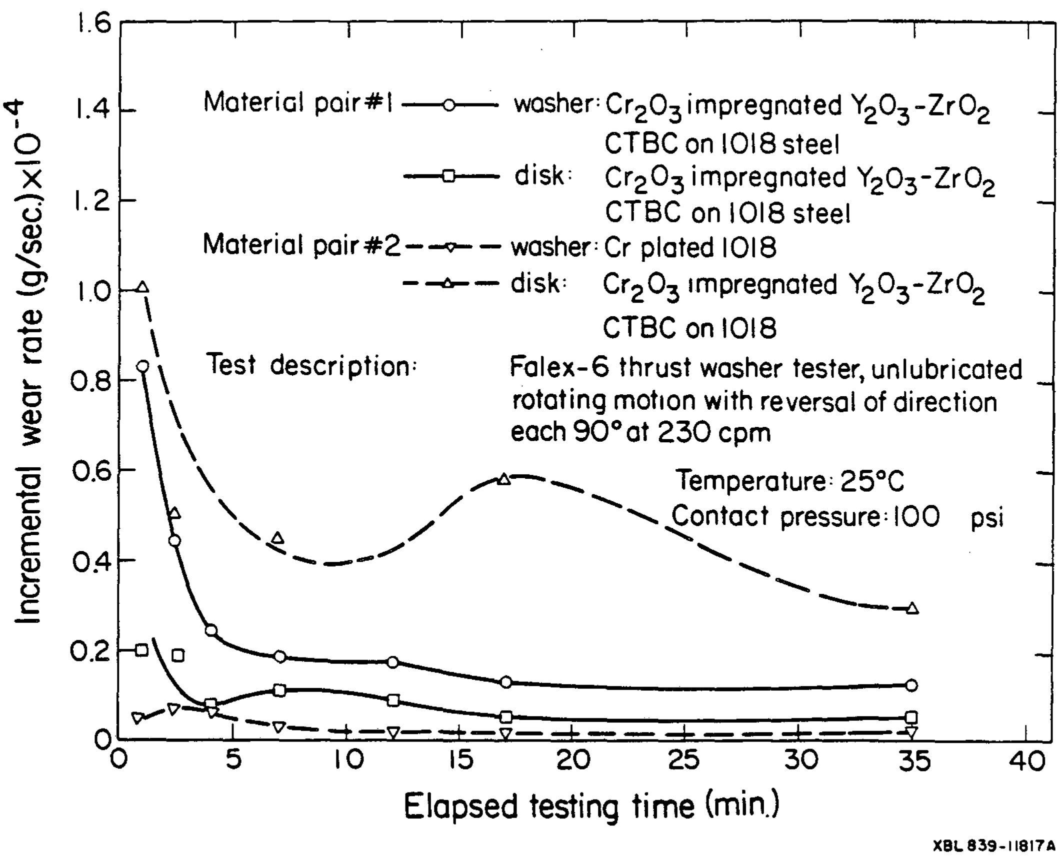

Fig. 15. Incremental wear rates of Cr plated 1018 steel and Cr_2O_3 impregnated Y_2O_3-ZrO_2 on washers and Cr_2O_3 impregnated Y_2O_3-ZrO_2 on discs of 1018 steel

DISTRIBUTION LIST

Wate Bakker
EPRI
3214 Hillview Avenue
P.O. Box 10412
Palo Alto, CA 94304

B.R. Banerjee
Ingersoll-Rand Company
P.O. Box 301
Princeton, NJ 08540

K.L. Baumert
Air Products & Chemicals, Inc.
P.O. Box 538
Allentown, PA 18105

S.M. Benford
NASA Lewis Research Center
21000 Brookpark Road
Cleveland, OH 41135

A.E. Biggs
Arco Chemicals
3801 W. Chester Pike
Newtown Square, PA 19073

R. Blickensderfer
Bureau of Mines
P.O. Box 70
Albany, OR 97321

R.A. Bradley, Manager
Fossil Energy Materials Program
Oak Ridge National Laboratory
P.O. Box X
Oak Ridge, TN 37830

Richard Brown
Materials Laboratory
Department of Chemical Engineering
University of Rhode Island
Kingston, RI 02881

DISTRIBUTION LIST cont'd

D.H. Buckley
NASA Lewis Research Center
21000 Brookpark Road
Cleveland, OH 41135

P.T. Carlson, Task Leader
Fossil Energy Materials Program
Oak Ridge National Laboratory
P.O. Box X
Oak Ridge, TN 37830

J. Carpenter
ECUT Program
Oak Ridge National Laboratory
P.O. Box X
Oak Ridge, TN 37830

J.P. Carr
Department of Energy, Office of Fossil Energy
FE-42 Mailstop 3222-GTN
Washington, DC 40525

Hans Conrad
Materials Engineering Department
North Carolina State University
Raleigh, NC 27659

P. Crook
Cabot Corporation
Technology Department
1020 W. Park Avenue
Kokomo, IN 46901

S.J. Dapkunas
Department of Energy, Office of Fossil Energy
Technical Coordination Staff FE-14
Mailstop C-156 GTN
Washington, DC 40525

DOE Technical Information Center
P.O. Box 62
Oak Ridge, TN 37830

W.A. Ellingson
Argonne National Laboratory
9700 South Cass Avenue
Argonne, IL 60439

DISTRIBUTION LIST cont'd

J. Gonzales
GTE
Chemical & Metallurgical Division
Hawes Street
Towanda, PA 18848

Å. Hammarsten
Teknikum
P.O. Box 534, S-751 21
Uppsala
SWEDEN

E. Haycock
Westhollow Research Center
Shell Development Company
P.O. Box 1380
Houston, TX 77001

J.M. Hobday
Department of Energy
Morgantown Energy Technology Center
P.O. Box 880
Morgantown, WV 26505

E.E. Hoffman, Manager
National Materials Program
Department of Energy
Oak Ridge Operations
P.O. Box E
Oak Ridge, TN 37830

J.A.C. Humphrey
Mechanical Engineering Department
University of California
Berkeley, CA 94720

I.M. Hutchings
University of Cambridge
Department of Metallurgy
Pembroke Street
Cambridge
ENGLAND

Sven Jansson
Stal-Laval Turbin AB
Finspong S-61220
SWEDEN

DISTRIBUTION LIST cont'd

R.R. Judkins
Fossil Energy Materials Program
Oak Ridge National Laboratory
P.O. Box X
Oak Ridge, TN 37830

M.K. Keshavan
Union Carbide Corporation
Coating Services Department
1500 Polco Street
Indianapolis, IN 46224

T. Kosel
University of Notre Dame
Dept. of Metallurgical Engineering
& Materials Science
Box E
Notre Dame, IN 46556

L. Lanier
FMC-Central Engineering Laboratory
1185 Coleman Avenue
Santa Clara, CA 95052

N.H. MacMillan
Pennsylvania State University
167 Materials Research Laboratory
University Park, PA 16802

P.K. Mehrotra
Kennemetal Inc.
1011 Old Salem Road
Greensburg, PA 15601

Ken Magee
Bingham-Williamette Co.
2800 N.W. Front Avenue
Portland, OR 97219

T. Mitchell
Case Western Reserve University
Department of Metallurgy
Cleveland, OH 44106

Fred Pettit
Dept. of Metallurgy & Materials Engineering
University of Pittsburgh
Pittsburgh, PA 15261

DISTRIBUTION LIST cont'd

R.A. Rapp
Metallurgical Engineering
116 W. 19th Avenue
The Ohio State University
Columbus, OH 43210

D.A. Rigney
Metallurgical Engineering
116 W. 19th Avenue
The Ohio State University
Columbus,OH 43210

A.W. Ruff
Metallurgy Division
National Bureau of Standards
B-266 Materials
Washington, DC 20234

Alberto Sagüés
IMMR - University of Kentucky
763 Anderson Hall
Lexington, KY 40506

Gordon Sargent
University of Notre Dame
Dept. of Metallurgical Engineering & Materials Science
Box E
Notre Dame, IN 46556

Paul Shewmon
Dept. of Metallurgical Engineering
116 W. 19th Avenue
Columbus, OH 43210

Gerry Sorell
EXXON Research & Engineering Company
P.O. Box 101
Florham Park, NJ 07932

John Stringer
University of California
Lawrence Berkeley Laboratory
Mailstop 62/203
Berkeley, CA 94720

Widen Tabakoff
Dept. of Aerospace Engineering
University of Cincinnati
Cincinnati, OH 45221

DISTRIBUTION LIST cont'd

Edward Vesely
IITRI
10 West 35th Street
Chicato, IL 60616

J.J. Wert
Metallurgy Department
Vanderbilt University
P.O. Box 1621, Sta. B
Nashville, TN 37235

J.C. Williams
Dept. of Metallurgy & Materials Science
Carnegie-Mellon University
Schenley Park
Pittsburgh, PA 15213

S. Wolf
Department of Energy
Basic Energy Sciences Office
Division of Materials Sciences
Washington, DC 20545

Ian Wright
Materials Science Division
Battelle Memorial Institute
505 King Avenue
Columbus, OH 43201

C.S. Yust
Metals and Ceramics Division
Oak Ridge National Laboratory
P.O. Box X
Oak Ridge, TN 37830

TECHNICAL INFORMATION DEPARTMENT
LAWRENCE BERKELEY LABORATORY
UNIVERSITY OF CALIFORNIA
BERKELEY, CALIFORNIA 94720